

Harnessing natural and mechanical airflows for surface-based atmospheric pollutant removal

Samuel D. Tomlinson^{1,2}, Aliko M. Tsopelakou^{1,2}, Tzia M. Onn^{1,2},
Steven R. H. Barrett¹, Adam M. Boies^{1,2} and Shaun D. Fitzgerald^{1,2}

¹Department of Engineering, University of Cambridge, Cambridge, United Kingdom

²Centre for Climate Repair, Cambridge, United Kingdom

March 18, 2025

Removal strategies for atmospheric pollutants are increasingly being considered to mitigate global warming and improve public health. However, surface-based removal techniques, such as sorption, catalysis and filtration, are often limited by pollutant transport and removal rate constraints. We evaluate the atmospheric pollutant transport to surfaces and assess the potential of surface-based removal technologies for applications in airflow through cities, HVAC systems and over vehicles. If these removal technologies are applied to their surfaces, cities, solar farms, HVAC systems and filters can achieve atmospheric pollutant removal rates that exceed 1 GtCO₂e annually (20-year GWP). Cities have the highest atmospheric pollutant removal potential, with estimates averaging 30 GtCO₂, 0.06 GtCH₄, 0.0001 GtPM_{2.5}, 0.007 GtNO_x annually. HVAC filters can achieve atmospheric pollutant removal costs as low as \$300 per tCO₂e removed when sorption or catalyst technologies are incorporated into their fibre sheets, outperforming the \$2000 per tCO₂e removal cost when these technologies are applied to city surfaces. This estimate is based on the literature values for these technologies' costs per square meter. However, our calculations indicate that optimising catalyst properties and surface coverage could lower the cost estimates to below \$100 per tCO₂e across these applications. These findings demonstrate that integrating surface-based pollutant removal technologies into infrastructure may offer a scalable pathway to advance climate and health objectives.

Greenhouse gases (GHGs) such as carbon dioxide (CO₂), methane (CH₄) and nitrous oxide (N₂O) continue to rise at significant rates, presenting sustainability and health challenges by accelerating climate change [22, 21]. In 2023, CO₂ levels surpassed 420 ppm, driven by fossil fuel use and deforestation, contributing to biodiversity loss and environmental degradation [35, 22]. The situation is compounded by CH₄ and N₂O, which, although emitted in smaller quantities, have global warming potentials (GWPs) 84 and 273 times that of CO₂ over a 20-year timescale. These potent GHGs are emitted by anthropogenic sources such as agriculture and fossil fuel processing [3, 56, 12, 38]. However, unlike CO₂, CH₄ and N₂O have biogenic sources that are difficult to control without disrupting agriculture and ecosystems. In addition to GHGs, atmospheric pollutants such as particulate matter (PM), sulphur dioxide (SO₂) and nitrogen oxides (NO_x) pose environmental and medical risks [27, 30]. PM, particularly particles smaller than 2.5 μm (PM_{2.5}), is a leading cause of respiratory and cardiovascular diseases, causing millions of premature deaths annually [47, 30, 33]. PM is emitted from anthropogenic sources, such as fossil fuel processing, and natural sources, like wildfires; SO₂ and NO_x have similar sources, but contribute to acid rain and ground-level ozone [7, 2, 5].

Given the diffuse nature of anthropogenic, biogenic and natural sources, coupled with the insufficient progress in emissions reductions, there is growing interest in atmospheric pollutant removal [35, 22, 12, 38, 30, 33, 7, 2, 5]. Atmospheric pollutant removal can generally be divided into two categories: surface-based approaches [39, 25, 26, 16, 23, 31, 57, 55], which rely on the interaction between pollutants and surfaces, and airborne methods, which use radicals or surface chemistry to

break down pollutants in the air [54, 36]. While airborne methods show promise, this study focuses on surface-based removal methods, given that these approaches are more widely explored and developed. Despite the interest in surface-based atmospheric pollutant removal [39, 25, 26, 16, 23, 31, 57, 55], the scale of potential removal remains unexplored. This study aims to assess the potential of various surface-based strategies by quantifying the scales at which pollutants can be removed from the atmosphere. Nonetheless, the methods developed here apply to other pollutants, offering a framework for quantifying the removal potential across contexts.

Direct air capture (DAC) technologies, often sorbent (e.g., amines) or solvent-based (e.g., potassium hydroxide), can capture CO₂ through chemical adsorption and absorption processes [39, 8]. For DAC, the fraction of pollutant molecules removed upon contact with the surface, known as the *removal efficiency*, ranges from 10⁻³ to 10⁰ [46]. However, this process requires substantial energy and involves high operational costs [29, 28]. Membrane-based systems, which separate CO₂ through selectively permeable barriers, offer greater energy efficiency than DAC, but face challenges related to initial costs and scalability [25]. Hence, while both methods show promise, their widespread application has been limited. In contrast, leveraging pre-existing natural and mechanical airflows, where the associated energy demands are already accounted for, may enable scalable and cost-effective surface-based methods for atmospheric pollutant removal.

Catalytic oxidation can convert CH₄ into CO₂ and water (H₂O), reducing its greenhouse impact; however, performance optimisation across environments remains challenging [26]. Reported CH₄ removal efficiencies for thermal, photo and elec-

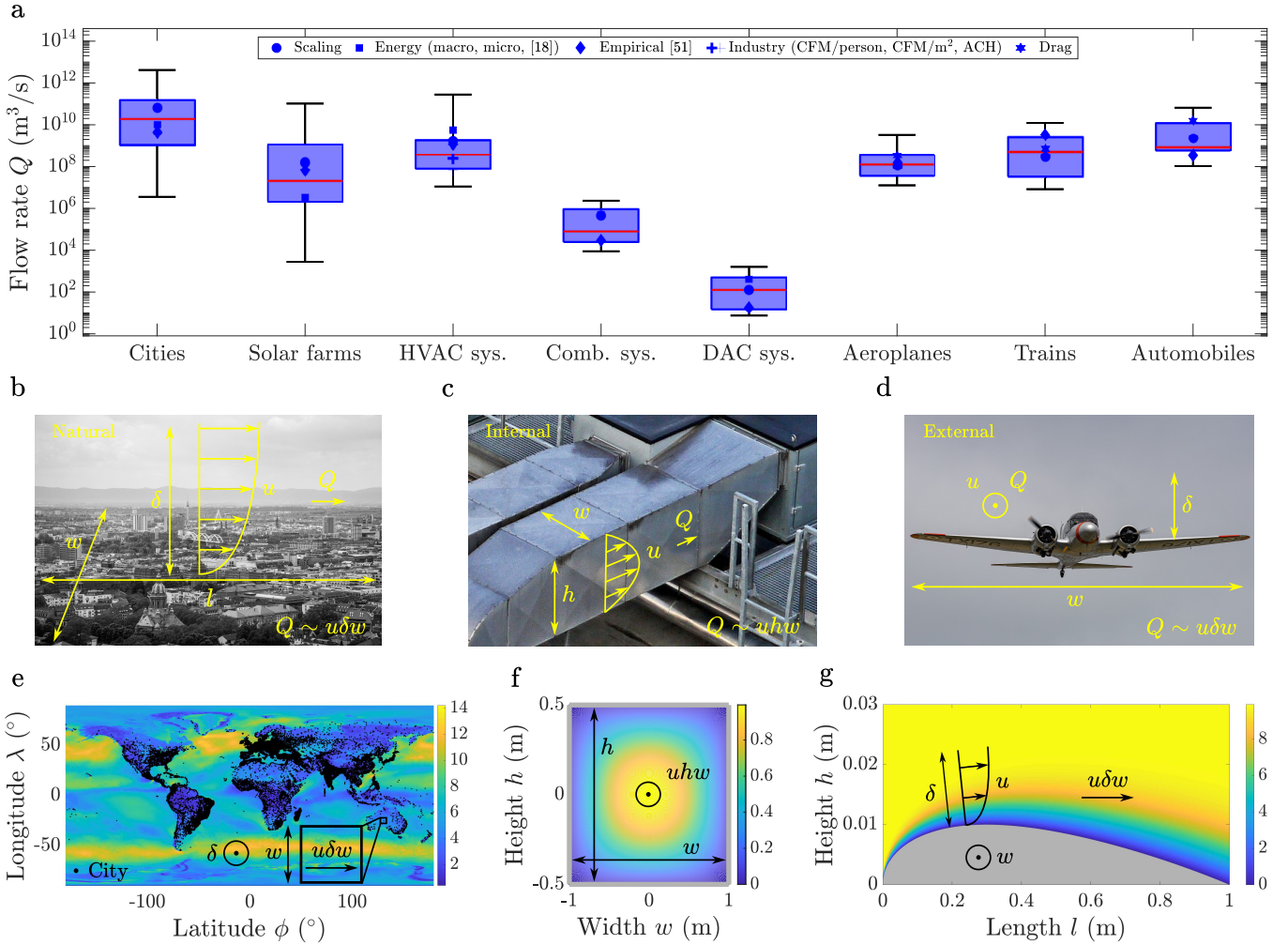


Figure 1: **Flow rates through global environments.** (a) Streamwise flow rates (Q) for natural airflows (e.g., cities, solar farms), internal airflows (e.g., HVAC, combustion, DAC systems) and external airflows (e.g., aeroplanes, trains, automobiles), with symbols denoting the methods used to estimate flow rates. Schematics of the velocity field (u), lengthscales (l , δ , w and h) and flow rate for a (b) city, (c) HVAC system and (d) aeroplane. (e) Global wind speed distribution, with city data highlighted in black. (f) Streamwise velocity profile through an HVAC system. (g) Boundary layer development across an aerofoil surface.

trocatalysts vary widely, from 10^{-10} to 10^0 , reflecting differences across catalysts and experimental conditions [50, 32]. Recent cost analyses suggest that using photocatalytic oxidation for atmospheric CH_4 removal is prohibitively expensive due to the high flow rates required for effective removal [36, 32, 18]. Alternatively, atmospheric radicals can break down CH_4 but at slow, condition-dependent rates [54, 36] and methanotrophic bacteria can remove CH_4 , albeit under controlled conditions [16]. This study examines catalytic oxidation as a strategy for atmospheric pollutant removal, exploring applications with varying surface fluxes and areas for scalable implementation.

Similar to CH_4 , N_2O can be removed via catalytic reduction, which converts N_2O into nitrogen (N_2) and oxygen (O_2) [36]. Another surface-based removal process is biological denitrification, where bacteria reduce N_2O to N_2 under anaerobic conditions [49].

High-efficiency particulate air (HEPA) filters are effective at capturing PM [23], alongside other methods such as electrostatic precipitators and adsorption materials such as activated carbon [31]. These technologies offer removal efficiencies of 10^{-1} to 10^0 [42], but require periodic regeneration or replacement due to saturation [24]. PM is also removed from

the atmosphere through dry (e.g., gravitational settling, surface absorption) and wet deposition (e.g., scavenging by rain), with removal rates varying by region and environmental conditions [45, 53, 15]. While these mechanisms for PM removal are well-established, our study will estimate how much $\text{PM}_{2.5}$ is removed from the atmosphere by filtration technologies and dry deposition via surface absorption, comparing these with the potential removal rates of other pollutants.

Similar to CH_4 and N_2O , SO_2 and NO_x can be removed using catalysis, which converts these pollutants into sulfuric acid (H_2SO_4) and N_2 [57]. Another removal method is scrubbing, where SO_2 and NO_x are removed from gas streams by passing them through chemically reactive liquid solutions [55].

In summary, although many surface-based pollutant removal methods exist (or are being proposed), they are often inefficient, energy-intensive and/or costly. Furthermore, the literature lacks an assessment of the potential scale of reductions achievable with surface-based atmospheric pollutant removal, despite the need for scalable solutions.

In this study, we examine approaches that could utilise the substantial volumes of air transported in urban areas, heating, ventilation and air conditioning (HVAC) systems, and transportation networks, where pollutants interact with surfaces to

enable their removal. Rather than focusing on the performance of specific surface-based technologies that remove specific pollutants, this study generally evaluates the scalability of atmospheric pollutant removal via surface-based interactions through transport limitations. We use a combination of theoretical models, empirical relations, global measurements and industry standards to estimate the atmospheric pollutant flow rate to the surfaces of various natural and mechanical systems. By leveraging removal efficiencies measured in the literature [46, 50, 32, 42], we assess the projected removal rates and technology costs for sorption, catalysis and filtration, for a range of environmental and flow conditions. We compare the potential atmospheric pollutant removal rates with intergovernmental targets and existing removal mechanisms, evaluating the scalability and cost-effectiveness of these surface-based technologies.

Results

Natural (e.g., cities, solar farms), internal (e.g., HVAC, combustion, DAC systems) and external environments (e.g., aeroplanes, trains, automobiles) offer significant opportunities for atmospheric pollutant removal. As shown in Fig. 1a and detailed in Supplementary Sec. 3, these environments consist of substantial airflow volumes that drive atmospheric pollutant fluxes to surfaces. Average streamwise flow rates are approximately 2×10^{10} m³/s through natural environments, 4×10^8 m³/s in internal systems and 8×10^8 m³/s around external systems. Theoretical predictions, empirical data, global measurements and industry standards provide a range of estimates in Fig. 1a, spanning from 3×10^6 to 4×10^{12} m³/s for cities, 1×10^7 to 3×10^{11} m³/s for HVAC systems and 1×10^8 to 7×10^{10} m³/s for automobiles. Key parameters, including length, surface area, velocity and the number of environments are summarised in Fig. 1b–g, Supplementary Tabs. 2–4 and Secs. 2.1–2.3. The parameter distributions not only capture uncertainty but reveal that surface area and airflow velocity are the dominant factors influencing pollutant removal efficiency across applications.

Surface fluxes of atmospheric pollutants

Fig. 2a shows normalised atmospheric pollutant fluxes to the surfaces of natural environments (columns 1–2) in cities and solar farms. GHG fluxes exceed other pollutant fluxes due to higher diffusivities and atmospheric concentrations (Fig. 2c). Atmospheric pollutant fluxes to surfaces are also influenced by length scales, with cities exhibiting average surface fluxes of 2×10^{-8} mol/m²s for CO₂, while solar farms achieve average surface fluxes of 2×10^{-7} mol/m²s for CO₂. Smaller length scales reduce the boundary layer thickness, which increases the turbulence intensity and improves the atmospheric pollutant transfer to surfaces. As a result, in these natural environments, atmospheric pollutant fluxes to surfaces are averaged across scales. Using empirical formulae detailed in the Methods, average atmospheric pollutant fluxes at the repeating unit scale (e.g., to the surface of individual buildings, 3×10^{-2} m⁻¹) are larger than those at the combined unit scale (e.g., to the surface of entire cities, 7×10^{-3} m⁻¹) due to steeper concentration gradients (Figs. 2a, d, e).

Figs. 2a–b highlight the enhanced atmospheric pollutant transport to the surfaces of internal airflows (columns 3–5) in

HVAC, combustion, DAC systems (Fig. 2a) and HVAC filters (Fig. 2b). Comparing HVAC, combustion and DAC systems, which show average surface fluxes of 7×10^{-5} , 2×10^{-4} and 6×10^{-5} mol/m²s for CO₂ in Fig. 2c, demonstrates that higher airflow velocities enhance atmospheric pollutant transport. The estimated value for DAC is comparable to 4×10^{-5} mol/m²s estimated in McQueen et al. [28]. At the duct wall, the rate at which pollutants move perpendicular to the surface (normal flux) depends on diffusion and is proportional to Dc/h (e.g., an average of 7×10^{-5} mol/m²s for CO₂, Fig. 2c, f), where D is the diffusivity of the pollutant, c is its concentration and h is the height of the channel. In contrast, for HVAC filters, the pollutant flux through the porous fibre sheet is proportional to $u_n c$ (e.g., an average of 3×10^{-3} mol/m²s for CO₂, Fig. 2c, g), where u_n is the airflow velocity through the fibre sheet. Since D and c are typically small relative to u_n and h , $u_n c$ is generally larger than Dc/h , highlighting the benefits of utilising advective over diffusive transport to improve atmospheric pollutant fluxes to surfaces.

Lastly, we evaluate the normalised atmospheric pollutant fluxes to the surfaces of external airflows over aeroplanes, trains and automobiles (columns 6–8, Fig. 2a). Automobiles demonstrate higher pollutant fluxes to surfaces than trains and aeroplanes (e.g., an average of 4×10^{-6} , 8×10^{-8} , 9×10^{-7} mol/m²s for CO₂, Fig. 2c), due to smaller characteristic lengths. However, aeroplanes generate more turbulent transport due to their higher velocities, resulting in a pollutant flux that is approximately 25% of the automobile flux across the entire surface.

Surface flow rates of atmospheric pollutants

Fig. 3 quantifies the flow rates of atmospheric CO₂, CH₄, PM_{2.5} and NO_x to all global surfaces. These flow rates are evaluated by multiplying the fluxes from Fig. 2 by the relevant surface area for each application (s in Fig. 2d–g) and the number of each application. Natural and internal airflows (columns 1, 3, 4) with extensive surface areas yield the highest atmospheric pollutant flow rates to their surfaces, e.g., an average of 30 GtCO₂/y for cities, 10 GtCO₂/y for HVAC systems and 4 GtCO₂/y for HVAC filters. Conversely, external airflows and small-surface-area internal systems (columns 5–8) show lower atmospheric pollutant flow rates to their surface, e.g., an average of 0.1 GtCO₂/y for aeroplanes, 0.7 GtCO₂/y for trains, 7×10^{-3} GtCO₂/y for combustion systems and 3×10^{-7} GtCO₂/y for DAC systems, despite external airflows exhibiting higher atmospheric pollutant fluxes to their surfaces in Fig. 2a–c.

Integrating surface-based pollutant removal technologies into global infrastructure is likely more readily achieved by incorporating technologies into newly-produced surfaces. Comparing atmospheric pollutant flow rates to total existing surfaces (Fig. 3) with annually produced surfaces (Supplementary Fig. 2), a decrease is observed across applications, with the reduction varying between applications. For example, solar farms and cities have average flow rates of 30 GtCO₂/y and 0.08 GtCO₂/y to their total surfaces. However, when accounting for annually produced surfaces, the average flow rate to new surfaces in cities (0.2 GtCO₂/y) is more significantly reduced than for solar farms (0.03 GtCO₂/y). This is largely driven by the global growth of solar farms, expanding at approximately 20% annually, compared with the 4% annual growth of cities.

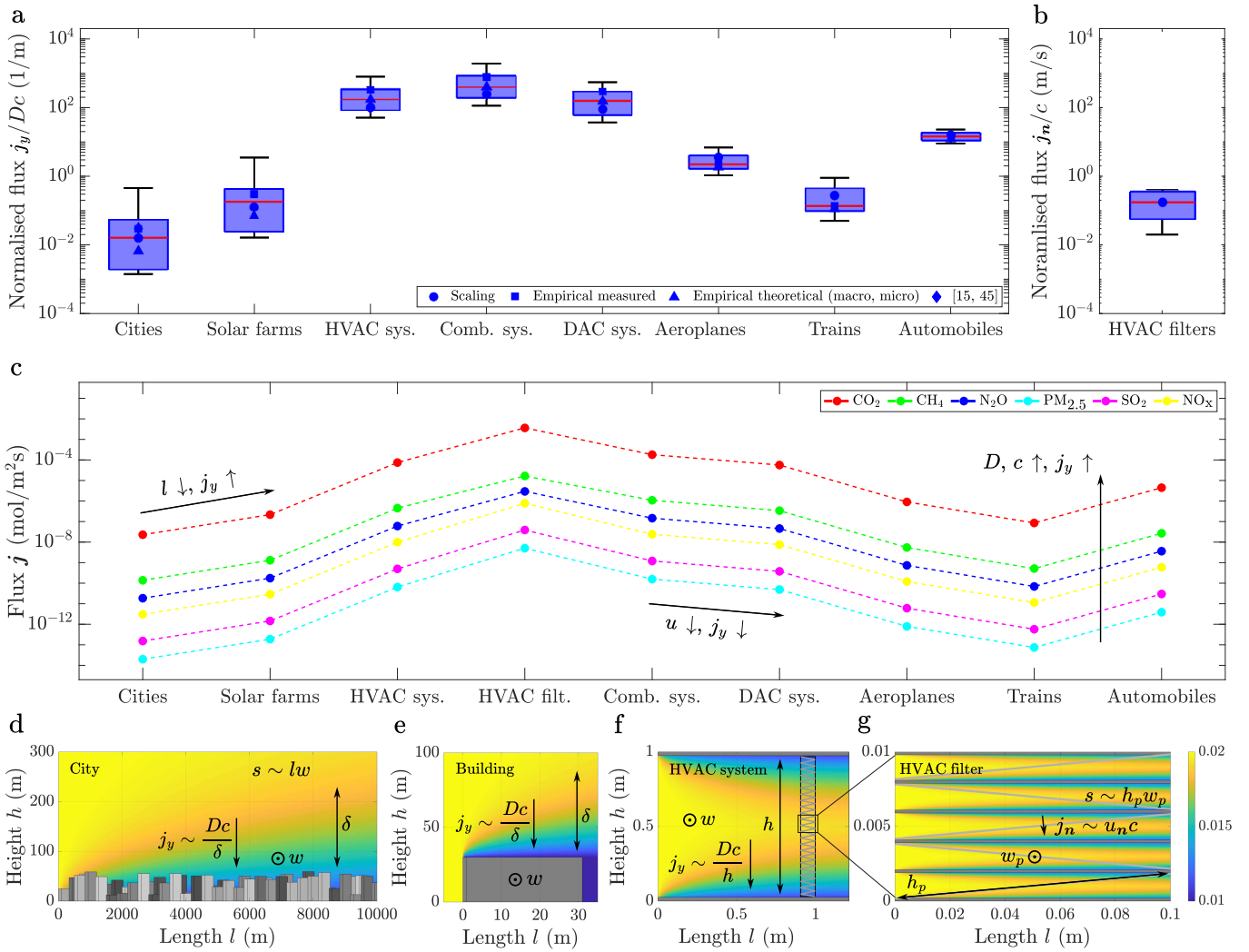


Figure 2: **Atmospheric pollutant fluxes to the surfaces of global environments.** (a) Atmospheric pollutant fluxes (j), normalised by diffusivity (D) and concentration (c), to the surfaces of natural airflows (e.g., cities, solar farms), internal airflows (e.g., HVAC, combustion, DAC systems) and external airflows (e.g., aeroplanes, trains, automobiles), with symbols representing the methods used to estimate fluxes. (b) Atmospheric pollutant fluxes, normalised by concentration, to the surfaces of HVAC filters. (c) Atmospheric pollutant fluxes to surfaces, averaged across the different methods, for CO₂, CH₄, N₂O, PM_{2.5}, SO₂ and NO_x. Example concentration boundary layer, velocities (u and u_n), lengths (l , δ , w , h , w_p , h_p) and normal pollutant flux to a (d) city surface, (e) building surface, (f) duct wall and (g) HVAC filter sheet.

Removal rates of atmospheric pollutants

Having established the atmospheric pollutant transport rates to the surfaces of various natural and mechanical environments, we assume ideal removal efficiencies and compare the potential atmospheric pollutant removal rates with the 1 GtCO₂e/y target (20–100-year GWP) [20]. This target appears feasible for cities, solar farms, HVAC systems, filters, aeroplanes, trains and automobiles, based on the potential atmospheric pollutant flow rates to existing surfaces (Fig. 3). When focusing only on potential atmospheric pollutant flow rates to annually produced surfaces (Supplementary Figs. 2), feasible applications narrow to cities, solar farms, HVAC systems and filters.

However, the removal efficiency is often suboptimal, falling short of the transport flux to surfaces. For example, DAC systems exhibit removal efficiencies around 10^{-1} [46], such that the average pollutant removal potential is 1 GtCO₂/y for HVAC systems. With 10 DAC systems removing, on average, around 10^3 tCO₂/y each [28], atmospheric removal rates are currently limited to approximately 10^{-5} GtCO₂/y (Fig. 3a).

CH₄ and N₂O present additional challenges due to their low atmospheric concentrations but can also achieve removal efficiencies around 10^{-1} [50]. However, most efficiency values are reported at elevated temperatures, with room temperature conversion rates still being an area of active research. When multiplied by the removal efficiency, cities, solar farms and HVAC systems have maximum pollutant removal potentials (20, 0.5, 2 GtCH₄/y respectively), which are greater than atmospheric oxidation (0.3 GtCH₄/y), providing a pathway that could surpass current emissions [9, 49]. PM_{2.5} is captured by HVAC filters which achieve removal efficiencies of around 10^0 [42], such that the average pollutant removal potential is 0.01 GtPM_{2.5}/y for HVAC filters. Atmospheric removal rates approach 4×10^{-6} GtPM_{2.5}/y (Fig. 3c), with a mean estimate of 100 million filters processing 100 m³/h at 99% efficiency [24].

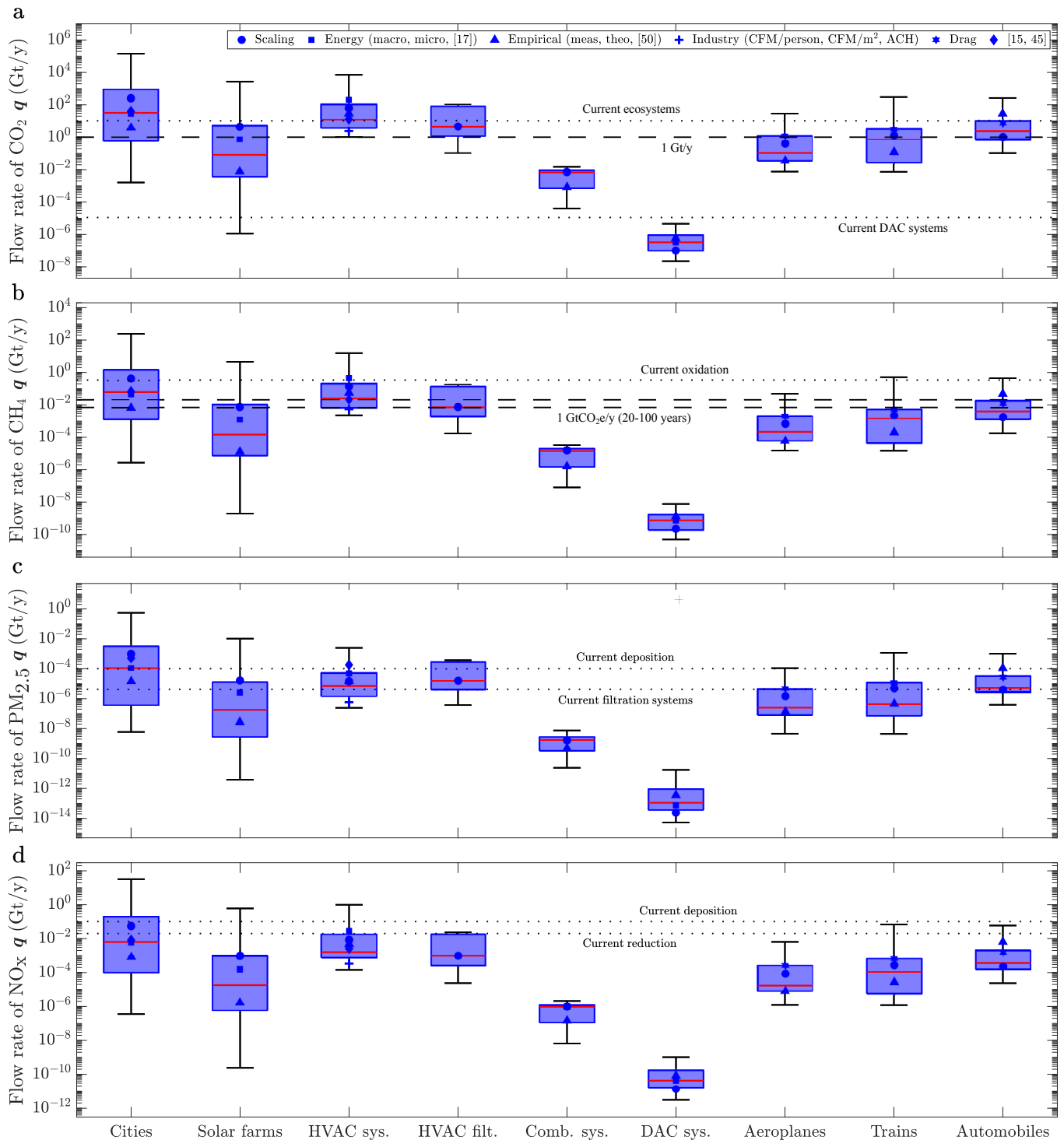


Figure 3: **Atmospheric pollutant flow rates to the surfaces of global environments.** Flow rates (q) of atmospheric (a) CO_2 , (b) CH_4 , (c) $\text{PM}_{2.5}$ and (d) NO_x to the total existing surfaces in natural (e.g., cities, solar farms), internal (e.g., HVAC systems, HVAC filters, combustion systems, DAC systems) and external (e.g., aeroplanes, trains, automobiles) environments, with symbols representing the methods used to estimate flow rates. Horizontal lines mark removal rates for atmospheric CO_2 , CH_4 , $\text{PM}_{2.5}$ and NO_x due to ecosystems, oxidation, deposition and reduction [14, 9, 49, 53, 10, 55, 57].

Cost analyses

Finally, we estimate the potential cost of scaling CO_2 -sorption and CH_4 -catalyst technologies, highlighting their capacity for atmospheric pollutant removal across natural and mechanical airflows. These surface-based technologies are selected as promising approaches for GHG removal, with estimated costs ranging from \$17 to \$73 per m^2 for CO_2 sorbents and \$14 to \$60 per m^2 for catalysts targeting CH_4 based

on [39, 29, 36, 18]. By contrast, atmospheric $\text{PM}_{2.5}$, as well as the oxidised forms of NO_x , are captured when they interact with surfaces through deposition. As shown in Fig. 3c–d, dry deposition rates of 1×10^{-4} $\text{GtPM}_{2.5}/\text{y}$ and 1×10^{-1} GtNO_x/y align with atmospheric pollutant flow rate estimates to urban surfaces [53, 10], contributing around 1–10% of global deposition.

To evaluate the potential cost-efficiency of each application,

Table 1: Cost of surface-based atmospheric pollutant removal in global environments. The potential removal rate of atmospheric CO₂ and CH₄ per year using a removal efficiency of 10⁻¹, surface area produced per year, technology cost per year based on cost per square meter [39, 29, 36, 18], cost per tonne of atmospheric CO₂ and CH₄ removed and cost per tonne of CO₂e removed for different natural and internal flows. Data for these natural and internal flows are divided into cities, solar farms, HVAC systems and filters that have potential removal rates of atmospheric CO₂ and CH₄ that exceed the 1 GtCO₂e/y target (20-year GWP) in Fig. 3.

Carbon dioxide (CO ₂)					
Environment	Rem. rate (t/y)	Surf. area (m ² /y)	Tech. cost (\$/y)	Rem. cost (\$/t)	Rem. cost (\$/tCO ₂ e)
Cities	[1 × 10 ³ , 3 × 10 ¹⁰]	[5 × 10 ⁹ , 1 × 10 ¹²]	[9 × 10 ¹⁰ , 7 × 10 ¹³]	[2 × 10 ³ , 9 × 10 ⁷]	[2 × 10 ³ , 9 × 10 ⁷]
Solar farms	[4 × 10 ² , 2 × 10 ¹⁰]	[5 × 10 ⁷ , 3 × 10 ¹¹]	[9 × 10 ⁸ , 2 × 10 ¹³]	[1 × 10 ³ , 2 × 10 ⁶]	[1 × 10 ³ , 2 × 10 ⁶]
HVAC systems	[1 × 10 ⁶ , 1 × 10 ¹⁰]	[3 × 10 ⁹ , 6 × 10 ¹⁰]	[5 × 10 ¹⁰ , 4 × 10 ¹²]	[4 × 10 ² , 5 × 10 ⁴]	[4 × 10 ² , 5 × 10 ⁴]
HVAC filters	[1 × 10 ⁶ , 2 × 10 ⁹]	[2 × 10 ⁷ , 8 × 10 ¹⁰]	[3 × 10 ⁸ , 6 × 10 ¹²]	[3 × 10 ² , 3 × 10 ³]	[3 × 10 ² , 3 × 10 ³]
Methane (CH ₄)					
Environment	Rem. rate (t/y)	Surf. area (m ² /y)	Tech. cost (\$/y)	Rem. cost (\$/t)	Rem. cost (\$/tCO ₂ e)
Cities	[5 × 10 ⁰ , 1 × 10 ⁸]	[5 × 10 ⁹ , 1 × 10 ¹²]	[7 × 10 ¹⁰ , 6 × 10 ¹³]	[6 × 10 ⁵ , 1 × 10 ¹⁰]	[7 × 10 ³ , 1 × 10 ⁸]
Solar farms	[2 × 10 ⁰ , 9 × 10 ⁷]	[5 × 10 ⁷ , 3 × 10 ¹¹]	[7 × 10 ⁸ , 2 × 10 ¹³]	[2 × 10 ⁵ , 4 × 10 ⁸]	[2 × 10 ³ , 5 × 10 ⁶]
HVAC systems	[9 × 10 ³ , 6 × 10 ⁷]	[3 × 10 ⁹ , 6 × 10 ¹⁰]	[4 × 10 ¹⁰ , 4 × 10 ¹²]	[7 × 10 ⁴ , 4 × 10 ⁶]	[8 × 10 ² , 5 × 10 ⁴]
HVAC filters	[5 × 10 ³ , 5 × 10 ⁶]	[2 × 10 ⁷ , 8 × 10 ¹⁰]	[3 × 10 ⁸ , 5 × 10 ¹²]	[6 × 10 ⁴ , 1 × 10 ⁶]	[6 × 10 ² , 1 × 10 ⁴]

we compare relative to atmospheric pollutant removal costs of \$100 per tCO₂e removed (20-year GWP), consistent with recommendations for GHG removal technologies [20]. We assume a removal efficiency of 10⁻¹ [46, 50, 32, 24], reflecting a realistic and optimistic average across surface-based removal technologies and pollutants. By dividing the estimated annual surface-based technology cost by the potential atmospheric pollutant removal rate, we derive the cost per tonne of CO₂e removed for each application in Tab. 1. Estimates across natural and internal environments exceed the \$100 per tCO₂e removed target. However, HVAC filters achieve potential costs as low as \$300 per tCO₂ removed for sorption and \$600 per tCO₂e removed for catalyst technologies. This lower cost for HVAC filters is attributed to the high atmospheric pollutant flux to their surface (e.g., an average of 0.003 mol/m²s for CO₂, Fig. 2c), which reduces the influence of surface area on the potential removal cost.

We explore the potential of different catalysts for atmospheric methane removal by varying material properties and surface coverage. Palladium (Pd) and magnesium (Mg) are considered, spanning material costs from \$10 to \$10⁴ per kg and densities from 1738 to 12023 kg/m³. We assume a catalyst particle size of 10⁻⁶m with 10% coverage. The cost per catalyst surface area is determined by multiplying the cost per kg by the catalyst mass and dividing by the catalyst surface area, yielding \$0.02 to \$120.2 per m² of catalyst. Fluxes are computed for the total surface area using Tab. 1 and adjusted for catalyst coverage. Therefore, we estimate the cost per ton of CO₂e removed to range from \$1.4 × 10⁵ to \$2 × 10⁶ for cities and \$3.2 to \$5.7 × 10³ for HVAC filters, the latter meeting the \$100 per tCO₂e target. Further reductions are possible by increasing catalyst coverage or reducing particle size, potentially bringing city-scale applications within target costs.

Discussion

The potential for removing low concentrations of atmospheric pollutants as a mitigation strategy for climate change and public health crises has yet to be fully explored. Surface-based removal technologies have been proposed as a scalable approach to achieving these reductions. For example, it has been shown that DAC may remove CO₂ from ambient air at scale [28], catalytic coatings in urban areas can reduce the concentration of volatile organic compounds (VOCs) and NO_x [43], and HEPA filters can lower PM levels [23]. To evaluate whether wider deployment is warranted, we have developed a framework to assess the potential scale of surface-based atmospheric pollutant removal, leveraging pre-existing airflows in cities, HVAC systems and transportation.

Surface-based pollutant removal technologies in cities, solar farms, HVAC systems and filters could achieve potential atmospheric pollutant removal rates exceeding 1 GtCO₂e per year (20–100 year GWP) [20], with optimisation for higher surface fluxes or lower materials costs potentially reducing the minimum cost estimate to under \$100 per tCO₂e. Building upon the existing capabilities of HVAC systems to remove PM and VOCs [23], by integrating other surface-based pollutant removal technologies, could enhance their cost-effectiveness and scalability. A similar integration of technologies was suggested during the COVID-19 pandemic, when HVAC systems were adapted to mitigate airborne viruses, using technologies such as UV-C light and antimicrobial coatings [48, 51]. This demonstrated the adaptability of HVAC systems and their potential for multifunctional air quality management to address broader environmental challenges. Furthermore, HVAC filters are regularly replaced, potentially making the maintenance of any surface-based removal technologies straightforward and allowing their performance to be sustained over time.

Refining pollutant removal models can not only enhance

the accuracy of predictions but also provide insights into optimisation. Adsorption/desorption models, such as Langmuir–Hinshelwood or Eley–Rideal, and multicomponent diffusion models, such as Maxwell–Stefan, can help identify conditions that maximise reaction rates [37, 4]. Similarly, dispersion models, including Gaussian plume, Eulerian and Lagrangian approaches, can enable placement of removal surfaces to enhance the removal efficiency [6]. Lastly, our analyses excluded energy consumption to focus on existing natural and mechanical airflows, assuming thin and smooth coatings with consistent flow resistance. However, rough coatings with increased surface area could enhance turbulence, flow rates to the surface and therefore removal efficiency.

Scaling surface-based atmospheric pollutant removal technologies presents challenges that must be addressed, including material degradation, surface contamination and infrastructure integration. While sorption systems generally maintain consistent pollutant removal efficiencies [46, 42], the catalytic removal of CH₄ is variable [50, 32] and may decrease over time or under varying conditions (e.g., relative humidity). Advances in materials and reaction mechanisms can improve these efficiencies and expand the applicability of catalysis. However, large-scale deployment of catalysts may introduce risks, such as the conversion of other species (e.g., VOCs) to more toxic forms.

These findings highlight the potential of integrating surface-based atmospheric pollutant removal technologies into urban and industrial systems to support climate action and protect public health.

Methods

Scaling theory

To characterise atmospheric pollutant transport dynamics across various systems, we define velocity (u , m/s), length (l , m) and surface area (s , m²) scales specific to each flow application (e.g., cities, HVAC systems, transport). We also estimate the number of occurrences (n) for each flow type to ensure realistic scaling for global estimations. The limitations of this scaling approach and additional context are provided in Supplementary Sec. 3.1.

The thickness of the turbulent ($Re > 10^5$) boundary layer (δ , m) is evaluated using $\delta = 0.4l/Re^{1/5}$, where the Reynolds number $Re = ul/\nu$ [41] and ν is the kinematic viscosity (m²/s). The normal pollutant flux j_y (mol/m²/s) at the surface is determined by the diffusive flux, $-Dc_y$, as the normal velocity at the surface is zero. The normal pollutant flux is simplified here using Fick’s law, which assumes diffusion driven solely by concentration gradients without accounting for molecular interactions or multicomponent effects. This normal pollutant flux depends on the diffusivity D (m²/s), concentration c (mol/m³) and the boundary layer thickness $\delta_c = \delta/Sc^{1/3}$ (m) [13], where the Schmidt number $Sc = \nu/D$. An effective diffusivity D_e (m²/s) is included to account for enhanced mixing, which alters pollutant transport rates [34].

Using these scales, the streamwise flow rate of pollutants Q (m³/s) through the boundary layer of each application is given by

$$Q \approx nu\delta l. \quad (1)$$

The normal flow rate of pollutants q_y (mol/s) to the surface of

each application is given by

$$q_y \approx \frac{ns(D + D_e)c}{\delta/Sc^{1/3}}. \quad (2)$$

The formulas in (1)–(2) provide a means to estimate atmospheric pollutant transport through, and to the surface of, global environments. As shown in Supplementary Fig. 1, we calculate the global streamwise flow rate through the boundary layers of the world’s cities (solar farms) using [17, 44, 11].

Empirical relationships

Empirical models can be used to link flow characteristics with the potential for pollutant removal [13]. These relationships have been applied in CH₄ and N₂O removal studies via photocatalysis [50, 36]. These relationships are evaluated using l , s and u , supplemented with measured values such as wall shear stresses (τ_w in kg/ms²), mass transfer coefficients (m_c in m/s) and heat transfer coefficients (h_c in W/m²K). A detailed discussion of these empirical relationships and their applications can be found in Supplementary Sec. 3.2.

Analogies exist between key dimensionless numbers: the Nusselt number ($Nu = h_c l/k$), the Sherwood number ($Sh = m_c l/D$) and the drag coefficient ($C_d = \tau_w/\rho u^2$), where k is the thermal conductivity (W/mK) and ρ is the fluid density (kg/m³) [13]. These analogies allow for the formulation of the normal pollutant flow rate to the surface of each application as follows

$$q_y \approx \frac{0.03Re^{4/5}Sc^{1/3}nsDc}{l}. \quad (3)$$

Following Tsopelakou *et al.* [50], we can use (3) to estimate the streamwise flow rate through each application as

$$Q \approx uA \approx lm_c P, \quad (4)$$

where P is the wetted perimeter and A is the cross-sectional area of the channel or boundary layer.

Fully-developed velocity and pollutant profiles

We employ established formulas to determine fully-developed velocity and pollutant profiles, including the Monin–Obukhov (M-O) similarity theory for natural airflows and approximate solutions of the Navier-Stokes equations for internal airflows, with explanations provided in Supplementary Sec. 3.3.

For external airflows over cities or solar farms, we utilise M-O similarity theory [41], which incorporates the effects of buoyancy and surface roughness under varying thermal conditions. The normal flow rate of pollutants to the surface of the environment is

$$q_y \approx \frac{ns(D + D_e)c}{\bar{h} \ln(\bar{h}/y_0)}, \quad (5)$$

where \bar{h} represents the average disturbance height and y_0 is the roughness length. For $y_0 = \delta^*$, where δ^* is the viscous sub-layer thickness, we recover the log-law profile. This log law applies to external airflows over smooth or mildly rough surfaces and can be used to calculate pollutant fluxes near vehicles [34].

For internal airflows within HVAC systems, we approximate solutions of the Navier-Stokes equations and boundary conditions [52]. The normal flow rate of pollutants to the channel walls is given by

$$q_y \approx \frac{ns(D + D_e)c}{h}, \quad (6)$$

where $2h$ is the channel diameter. For internal airflows through HVAC filters, we adjust the velocity from the duct flow (with velocity u , diameter $2h$ and cross-channel area A) to the pleat flow (with velocity u_n , diameter $2h_p$, filter sheet area A_p , number m). We apply the principle of mass conservation to match average velocities, leading to $Au \approx mA_p u_n$. The flow rate of pollutants to the pleat channel walls is

$$q_y \approx \frac{nms(D + D_e)c}{h_p}. \quad (7)$$

The flow rate of pollutants to the fibre sheet is

$$q_n \approx nmA_p E u_n c, \quad (8)$$

where E is the collection efficiency, related to the permeability and porosity of the filter medium [19].

Energy, power and drag measurements

We now outline formulas to determine the flow rate based on energy, power and drag measurements. More details are given in Supplementary Sec. 3.4.

For external flows over urban areas or solar farms, we establish a control volume with a length l and height δ . In the case of uni-directional, steady-state flow over a surface with a heat flux ϕ (W/m^2), energy conservation dictates that the energy entering the control volume must balance with the energy exiting it [13]. This relationship can be expressed as

$$Q \approx \frac{ns\phi}{\rho c_p \Delta T}, \quad q_y \approx \frac{Ql(D + D_e)c}{\delta^2 u}, \quad (9)$$

where c_p ($\text{m}^2/\text{s}^2\text{K}$) is the specific heat capacity of air at constant pressure and ΔT (K) is the temperature difference between the surface and the surrounding atmosphere. The flow rates are related using the scaling theory discussed in Supplementary Sec. 3.1, such that $Ql(D + D_e)c/(\delta^2 u) \sim (u\delta)l(D + D_e)c/(\delta^2 u) \sim l(D + D_e)c/\delta \sim q_y$.

In the context of internal flow through HVAC systems, the total power consumed by the fans denoted as P (kW) and the specific fan power (SFP) ($\text{W}/\text{m}^2/\text{s}$), can be utilised to evaluate the streamwise flow rate through the duct as follows

$$Q \approx \frac{LP}{\text{SFP}}, \quad (10)$$

where L is the leakage factor [40].

For external airflows acting on transportation systems, the streamwise flow rate through the boundary layer can be estimated using the drag force acting on the aeroplane, train or automobile [52]. This is expressed by the equation

$$Q \approx \frac{2nF_d}{\rho u C_d}, \quad (11)$$

where F_d (N) is the drag force.

Industry standards

For internal airflows through HVAC ducting, the streamwise flow rate can be evaluated using three estimates [1]. First, Q can be expressed in terms of the cubic feet per minute per person (CFM_{pp} , ft^3/min), given by

$$Q \approx L\text{CFM}_{\text{pp}} n_{\text{pp}}, \quad (12)$$

where n_{pp} (–) is the total number of occupants in the building. Second, Q can be calculated based on the CFM per unit area (CFM_{pm^2} , $\text{ft}^3/\text{min}/\text{m}^2$), described by the equation

$$Q \approx L\text{CFM}_{\text{pm}^2} a, \quad (13)$$

where a (m^2) is the total floor area of the building. Finally, Q can be assessed using the air changes per hour (ACH, s), given by

$$Q \approx L\text{ACH}v, \quad (14)$$

where v (m^3) is the volume of air within the building.

References

- [1] American Society of Heating, Refrigerating and Air-Conditioning Engineers. *ASHRAE Handbook: Fundamentals*. ASHRAE, Atlanta, GA, 2024 edition, 2024.
- [2] P. Amoatey, H. Omidvarborna, M. S. Baawain, and A. Al-Mamun. Emissions and exposure assessments of SO_x , NO_x , $\text{PM}_{10/2.5}$ and trace metals from oil industries: A review study (2000–2018). *Process Saf. Environ. Prot.*, 123:215–228, 2019.
- [3] P. Balcombe, J. F. Speirs, N. P. Brandon, and A. D. Hawkes. Methane emissions: choosing the right climate metric and time horizon. *Environ. Sci. Process. Impacts*, 20(10):1323–1339, 2018.
- [4] R. Byron Bird, W. E. Stewart, and E. N. Lightfoot. *Transport Phenomena*. Wiley & Sons, New York, 4th edition, 2006.
- [5] T. Boningari and P. G. Smirniotis. Impact of nitrogen oxides on the environment and human health: Mn-based materials for the NO_x abatement. *Curr. Opin. Chem. Eng.*, 13:133–141, 2016.
- [6] R. E. Britter and S. R. Hanna. Flow and dispersion in urban areas. *Annu. Rev. Fluid Mech.*, 35(1):469–496, 2003.
- [7] J. N. Cape, D. Fowler, and A. Davison. Ecological effects of sulfur dioxide, fluorides, and minor air pollutants: recent trends and research needs. *Environ. Int.*, 29(2-3):201–211, 2003.
- [8] R. Custelcean. Direct air capture of CO_2 using solvents. *Annu. Rev. Chem. Biomol. Eng.*, 13(1):217–234, 2022.
- [9] E. J. Dlugokencky, E. G. Nisbet, R. Fisher, and D. Lowry. Global atmospheric methane: budget, changes and dangers. *Philos. Trans. R. Soc. A*, 369(1943):2058–2072, 2011.
- [10] A. J. Dore, M. Vieno, Y. S. Tang, U. Dragosits, A. Dosio, K. J. Weston, and M. A. Sutton. Modelling the atmospheric transport and deposition of sulphur and nitrogen over the united kingdom and assessment of the influence of SO_2 emissions from international shipping. *Atmospheric Environment*, 41:2355–2367, 2007.
- [11] S. Dunnett, A. Sorichetta, G. Taylor, and F. Eigenbrod. Harmonised global datasets of wind and solar farm locations and power. *Sci. Data*, 7(1):130, 2020.
- [12] P. Forster, T. Storelvmo, K. Armour, W. Collins, J.-L. Dufresne, D. Frame, D. Lunt, T. Mauritsen, M. Palmer, M. Watanabe, M. Wild, and H. Zhang. *The Earth’s energy budget, climate feedbacks, and climate sensitivity*, chapter 7. Cambridge University Press, 2021.
- [13] P. Frank. *Incropera’s principles of heat and mass transfer*, 2017.
- [14] P. Friedlingstein, M. O’Sullivan, M. W. Jones, R. M. Andrew, L. Gregor, J. Hauck, C. Le Quéré, I. T. Luijkx, A. Olsen, G. P. Peters, et al. Global carbon budget 2022. *Earth Syst. Sci. Data*, 14(11):4811–4900, 2022.

- [15] M. Giardina, A. Donateo, P. Buffa, D. Contini, A. Cervone, C. Lombardo, and F. Rocchi. Atmospheric dry deposition processes of particles on urban and suburban surfaces: Modelling and validation works. *Atmospheric Environment*, 214:116857, 2019.
- [16] S. Guerrero-Cruz, A. Vaksmaa, M. A. Horn, H. Niemann, M. Pijuan, and A. Ho. Methanotrophs: discoveries, environmental relevance, and a perspective on current and future applications. *Front. Microbiol.*, 12:678057, 2021.
- [17] H. Hersbach, B. Bell, P. Berrisford, S. Hirahara, A. Horányi, J. Muñoz-Sabater, J. Nicolas, C. Peubey, R. Radu, D. Schepers, et al. Era5 reanalysis (single levels), 2017. Copernicus Climate Change Service (C3S) Data Store (CDS), accessed 2024. <https://cds.climate.copernicus.eu/datasets/reanalysis-era5-single-levels>.
- [18] C. Hickey and M. Allen. Economics of enhanced methane oxidation relative to carbon dioxide removal. *Environ. Res. Lett.*, 19(6):064043, 2024.
- [19] W. C. Hinds and Y. Zhu. *Aerosol Technology: Properties, Behavior, and Measurement of Airborne Particles*. John Wiley & Sons, 2022.
- [20] Intergovernmental Panel on Climate Change. Climate change 2023: Synthesis report. Technical report, IPCC, 2023. Accessed: 2024-10-11.
- [21] M. W. Jones, G. P. Peters, T. Gasser, R. M. Andrew, C. Schwingshackl, J. Gutschow, R. A. Houghton, P. Friedlingstein, J. Pongratz, and C. Le Quééré. National contributions to climate change due to historical emissions of carbon dioxide, methane, and nitrous oxide since 1850. *Sci. Data*, 10(1):155, 2023.
- [22] P. Kumar. Climate change and cities: challenges ahead. *Front. Sustain. Cities*, 3:645613, 2021.
- [23] H. Liu, C. Cao, J. Huang, Z. Chen, G. Chen, and Y. Lai. Progress on particulate matter filtration technology: basic concepts, advanced materials, and performances. *Nanoscale*, 12(2):437–453, 2020.
- [24] S. D. Lowther, W. Deng, Z. Fang, D. Booker, J. D. Whyatt, O. Wild, X. Wang, and K. C. Jones. Factors affecting real-world applications of hepa purifiers in improving indoor air quality. *Environ. Sci. Adv.*, 2:235–246, 2023.
- [25] P. Luis, T. Van Gerven, and B. Van der Bruggen. Recent developments in membrane-based technologies for co2 capture. *Prog. Energy Combust. Sci.*, 38(3):419–448, 2012.
- [26] J. H. Lunsford. Catalytic conversion of methane to more useful chemicals and fuels: a challenge for the 21st century. *Catal. Today*, 63(2-4):165–174, 2000.
- [27] I. Manisalidis, E. Stavropoulou, A. Stavropoulos, and E. Bezirtzoglou. Environmental and health impacts of air pollution: a review. *Front. Public Health*, 8:14, 2020.
- [28] N. McQueen, K. V. Gomes, C. McCormick, K. Blumanthal, M. Pisciotta, and J. Wilcox. A review of direct air capture (dac): scaling up commercial technologies and innovating for the future. *Prog. Energy*, 3(3):032001, 2021.
- [29] N. McQueen, P. Psarras, H. Pilorgé, S. Liguori, J. He, M. Yuan, C. M. Woodall, K. Kian, L. Pierpoint, J. Jurewicz, et al. Cost analysis of direct air capture and sequestration coupled to low-carbon thermal energy in the united states. *Environ. Sci. Technol.*, 54(12):7542–7551, 2020.
- [30] World Health Organization et al. *WHO global air quality guidelines: particulate matter (PM2.5 and PM10), ozone, nitrogen dioxide, sulfur dioxide and carbon monoxide*. World Health Organization, 2021.
- [31] K. R. Parker. Why an electrostatic precipitator? In *Applied electrostatic precipitation*, pages 1–10. Springer, 1997.
- [32] L. Pennacchio, M. K. Mikkelsen, M. Krogsbøll, M. M. J. W. van Herpen, and M. Johnson. Physical and practical constraints on atmospheric methane removal technologies. *Environ. Res. Lett.*, 2024.
- [33] G. Polichetti, S. Cocco, A. Spinali, V. Trimarco, and A. Nunziata. Effects of particulate matter (pm10, pm2.5 and pm1) on the cardiovascular system. *Toxicol.*, 261(1-2):1–8, 2009.
- [34] S. B. Pope. *Turbulent Flows*. Cambridge University Press, 2000.
- [35] I. C. Prentice, G. D. Farquhar, M. J. R. Fasham, M. L. Goulden, M. Heimann, V. J. Jaramillo, H. S. Khesghi, C. Le Quééré, R. J. Scholes, D. W. R. Wallace, et al. The carbon cycle and atmospheric carbon dioxide. *Climate Change 2001: The Scientific Basis, Intergovernmental Panel on Climate Change*, 2001.
- [36] R. Randall, R. B. Jackson, and A. Majumdar. Cost modeling of photocatalytic decomposition of atmospheric methane and nitrous oxide. *Environ. Res. Lett.*, 19(6):064015, 2024.
- [37] G. Rothenberg. *Catalysis: Concepts and Green Applications*. John Wiley & Sons, 2017.
- [38] F. S. Rowland. Stratospheric ozone depletion. *Philos. Trans. R. Soc. B Biol. Sci.*, 361(1469):769–790, 2006.
- [39] E. S. Sanz-Pérez, C. R. Murdock, S. A. Didas, and C. W. Jones. Direct capture of co2 from ambient air. *Chem. Rev.*, 116(19):11840–11876, 2016.
- [40] P. G. Schild and M. Mysen. Recommendations on specific fan power and fan system efficiency. *Tech. Note AIVC*, 65, 2009.
- [41] H. Schlichting and K. Gersten. *Boundary-layer theory*. Springer, 2016.
- [42] T. Schroth. New hepa/ulpa filters for clean-room technology. *Filtr. Separ.*, 33:245–244, 1996.
- [43] K. W. Shah and W. Li. A review on catalytic nanomaterials for volatile organic compounds voc removal and their applications for healthy buildings. *Nanomaterials*, 9(6):910, 2019.
- [44] SimpleMaps. World cities database, 2024. Accessed: 2024-10-17.
- [45] M. R. Sippola and W. W. Nazaroff. Particle deposition from turbulent flow: Review of published research and its applicability to ventilation ducts in commercial buildings. Technical Report LBNL–51432, Lawrence Berkeley National Laboratory, 2002.
- [46] J. K. Soeherman, A. J. Jones, and P. J. Dauenhauer. Overcoming the entropy penalty of direct air capture for efficient gigatonne removal of carbon dioxide. *ACS Eng. Au*, 3(2):114–127, 2023.
- [47] B. S. Sosa, A. Porta, J. E. C. Lerner, R. B. Noriega, and L. Masolo. Human health risk due to variations in pm10-pm2.5 and associated pahs levels. *Atmos. Environ.*, 160:27–35, 2017.
- [48] G. M. Thornton, B. A. Fleck, N. Fleck, E. Kroeker, D. Dandnayak, L. Zhong, and L. Hartling. The impact of heating, ventilation, and air conditioning design features on the transmission of viruses, including the 2019 novel coronavirus: A systematic review of ultraviolet radiation. *PLoS One*, 17(4):e0266487, 2022.

- [49] H. Tian, N. Pan, R. L. Thompson, J. G. Canadell, P. Suntharalingam, P. Regnier, E. A. Davidson, M. Prather, P. Ciais, M. Muntean, et al. Global nitrous oxide budget 1980–2020. *Earth Syst. Sci. Data Disc.*, 2023:1–98, 2023.
- [50] A. M. Tsopeleakou, J. Stallard, A. T. Archibald, S. Fitzgerald, and A. M. Boies. Exploring the bounds of methane catalysis in the context of atmospheric methane removal. *Environ. Res. Lett.*, 19(5):054020, 2024.
- [51] R. Watson, M. Oldfield, J. A. Bryant, L. Riordan, H. J. Hill, J. A. Watts, M. R. Alexander, M. J. Cox, Z. Stamatakis, D. J. Scurr, et al. Efficacy of antimicrobial and anti-viral coated air filters to prevent the spread of airborne pathogens. *Scientific Reports*, 12(1):2803, 2022.
- [52] F. M. White and H. Xue. *Fluid mechanics*, volume 3. McGraw-Hill, 2003.
- [53] Y. Wu, J. Liu, J. Zhai, L. Cong, Y. Wang, W. Ma, Z. Zhang, and C. Li. Comparison of dry and wet deposition of particulate matter in near-surface waters during summer. *PLoS One*, 13(6):e0199241, 2018.
- [54] D. J. Wuebbles and K. Hayhoe. Atmospheric methane and global change. *Earth-Sci. Rev.*, 57(3-4):177–210, 2002.
- [55] Y. Xu, R. H. Williams, and R. H. Socolow. China’s rapid deployment of so₂ scrubbers. *Energy Environ. Sci.*, 2:459–465, 2009.
- [56] R. O. Yusuf, Z. Z. Noor, A. H. Abba, M. A. A. Hassan, and M. F. M. Din. Methane emission by sectors: a comprehensive review of emission sources and mitigation methods. *Renew. Sustain. Energy Rev.*, 16(7):5059–5070, 2012.
- [57] S. Zhao, J. Peng, R. Ge, S. Wu, K. Zeng, H. Huang, K. Yang, and Z. Sun. Research progress on selective catalytic reduction (scr) catalysts for nox removal from coal-fired flue gas. *Fuel Process. Technol.*, 236:107432, 2022.